ChemCatChem

Research Article
doi.org/10.1002/cctc.202400908

Chemistry Europe
European Chemical Societies Publishing

www.chemcatchem.org

Yeast Surface Display Enables One-Step Production and Immobilization of Unspecific Peroxygenases

Niklas Teetz,[a, b] Selina Lang,[b] Andreas Liese,[c] and Dirk Holtmann*[a]

Unspecific peroxygenases (UPOs) are regarded as a "dream catalyst" for selective oxyfunctionalization reactions like oxygenations. We present the display of the model UPO r*Aae*UPO (PaDa–I) on the cell surface of the heterologous production host *Komagataella phaffii* as a one-step production and immobilization process. The coding sequence for PaDa–I was combined with genes coding for cell wall proteins from *Saccharomyces cerevisiae* and transformed into *K. phaffii*. The fusion proteins were compared among each other and with secreted, free PaDa–I. One system in particular, a C-terminal fusion of PaDa–I and Sag1 yielded near identical activity per volume culture broth to the secreted PaDa–I with ~90% of the activity being at the cell wall. The surface display simplifies downstream processing and includes immobilization on a cheap, retainable and replaceable matrix, that is the production host itself. The enzymes remained active in a repeated batch process for 10 batches and 200 h of catalysis.

Introduction

Unspecific peroxygenases (UPOs, EC 1.11.2.1) are a group of fungal heme thiolate enzymes, catalyzing a variety of selective oxyfunctionalization reactions like hydroxylations, epoxidations and oxygenations. They are regarded as a "dream catalyst" due to their high activities, robustness and independence from reduced nicotinamide cofactors and complex electron transport chains by using hydrogen peroxide as only cofactor.[1] They can be produced heterologously by the commonly used production yeast *Komagataella phaffii* (*Pichia pastoris*).

The potential areas of application are manyfold and include pharmaceutical and chemical industry as well as valorization of waste streams. The broad substrate scope of UPOs includes pharmaceuticals like propranolol, diclofenac[2] or the resveratrol analogue 4,4′-dihydroxy-*trans*-stilbene,[3] as well as several platform and waste stream chemicals like linear and cyclic alkanes,[4] alkylbenzenes[5] or fatty acids.[6] Although the catalyzed reactions are highly interesting and production of as well as catalysis with UPOs has recently been shown on pilot scale,[7] industrial application of oxygenases, including UPOs, remains uncommon.[1a] The main cause for this is the high cost associated with production and downstream processing of the biocatalyst which limits the worthwhile products to high value fine chemicals and pharmaceuticals. Depending on the needed purity of the enzyme, multiple downstream processing stages are required after the enzyme production. Although UPOs are typically secreted and no cell disruption is needed, centrifugation, microfiltration, ultrafiltration and diafiltration and chromatographic purification steps are required for most applications. This downstream processing contributes to the price of the enzyme by adding production time, material cost and most importantly limiting the yield which has been demonstrated by Tonin and coworkers for a 2500 L fermentation.[7a]

An immobilization of UPOs is desirable for repeated or continuous use of the enzyme to maximize the amount of catalytic turnovers per biocatalyst and thereby reducing the cost per turnover. Some immobilization strategies, that rely on specific affinities of the carrier to the enzyme, can also reduce downstream processing by immobilizing the enzyme out of crude cultivation supernatant. Such immobilization has been shown for a hexahistidine-tagged variant of the UPO from *Agrocybe aegerita* (PaDa–I variant).[8] However, enzyme immobilization itself is often connected to high cost and time commitment or activity loss of the enzyme, depending on the immobilization strategy.[9] This is certainly true for PaDa–I as multiple immobilization strategies have been explored but activity yields remain below 10%. In 2019, the group that initially developed the PaDa–I variant of *Aae*UPO, immobilized it by changing the serine 221 residue on its surface to a cysteine and using a directed unique-point covalent immobilization strategy based on the SH functional group of the cysteine. While the bond was very stable, the S221 C variant of PaDa–I showed 40% less secretion during production and the immobilization yield was only 15% for the two tested carriers.[10] In the before mentioned work of Bormann and coworkers,[8] his-tag

[a] *N. Teetz, D. Holtmann*
Institute of Process Engineering in Life Sciences 2 - Electrobiotechnology, Karlsruhe Institute of Technology, Fritz-Haber-Weg 4, 76131 Karlsruhe, Germany
E-mail: dirk.holtmann@kit.edu

[b] *N. Teetz, S. Lang*
Institute for Bioprocess Engineering and Pharmaceutical Technology – Intensification of Bioprocesses, University of Applied Sciences Gießen, Wiesenstraße 14, 35390 Gießen, Germany

[c] *A. Liese*
Institute of Technical Biocatalysis, Hamburg University of Technology, Denickestraße 15, 21073 Hamburg, Germany

Supporting information for this article is available on the WWW under https://doi.org/10.1002/cctc.202400908

immobilization itself was comparatively efficient with a yield of 53 to 78% but the his-tag reduced the enzymes activity to 10% of the non-tagged version, resulting in an overall activity yield of 5–8%. Recently, Hobisch and coworkers used PaDa–I immobilized on an amino methacrylate (ECR8315F) carrier in a rotating bed reactor to great success. The immobilization yield was 52% but the enzymes specific activity was only 1.7% of the free enzymes specific activity described by Molina-Espeja and coworkers.[11] An in-depth study of many carrier-bound immobilization methods for both his_6-tagged and non-tagged PaDa–I by De Santis and coworkers confirm the dilemma of either low activity yield or medium to high activity yield with a less active (his-tagged) enzyme[12] and the authors emphasize the importance of a good activity yield in a recent study.[13] For a comprehensible comparison, see supporting information Table SI 1.

Clearly, a cheap immobilization method for UPOs with satisfactory activity yields is necessary for the establishment of industrial UPO-based processes. Especially immobilization from crude culture broth or with minimal downstream processing steps after cultivation is desirable to reduce the cost of immobilized biocatalyst.

Here, we used yeast surface display (YSD) systems to immobilize the model UPO *Aae*UPO (PaDa–I variant) on the cells of its heterologous production host *K. phaffii*. YSD has been demonstrated for various enzyme classes including oxidoreductases,[14] hydrolases,[15] isomerases[16] and ligases,[17] often improving catalytic parameters of the displayed enzyme. The general principles of YSD and a comprehensive overview over the different anchor systems, used yeast strains and optimization approaches are excellently summarized in the reviews by Andreu and Olmo and Ye and coworkers.[18] In short, the gene of interest is combined with genes or partial genes, coding for cell wall proteins as attachment anchor and signal peptides, to direct the fusion protein to the outside of the cell and attach to the cell wall. The anchors attachment mechanism, the resulting distance of the enzyme of interest to the cell and possible interactions between the anchor and the enzyme of interest can affect the enzymes activity and stability. To the authors knowledge, YSD of UPOs has not been reported before but has the potential to both drastically shorten downstream processing and be used as immobilization method.

The coding sequence for PaDa–I was combined with genes coding for a variety of cell wall proteins, originally responsible for flocculation, cell contact during mating or cell wall stability in *Saccharomyces cerevisiae*. The fusion-genes were transformed into *K. phaffii* via an integration vector for production and comparison of the fusion proteins among each other and with secreted, free PaDa–I. An activity screening and biochemical characterization for the parameters temperature, pH and organic solvent concentration were done to identify the most promising YSD system. Subsequently, this system and two variants of it (Scheme 1), bearing a Strep-tag®II or Gfp-tag were used for detailed analysis of key immobilization parameters and finally, the effectiveness of the surface display as immobilization method was demonstrated by a repeated batch experiment, where the cells were recovered over 13 batches. This work presents a cheap and extremely effective UPO immobilization

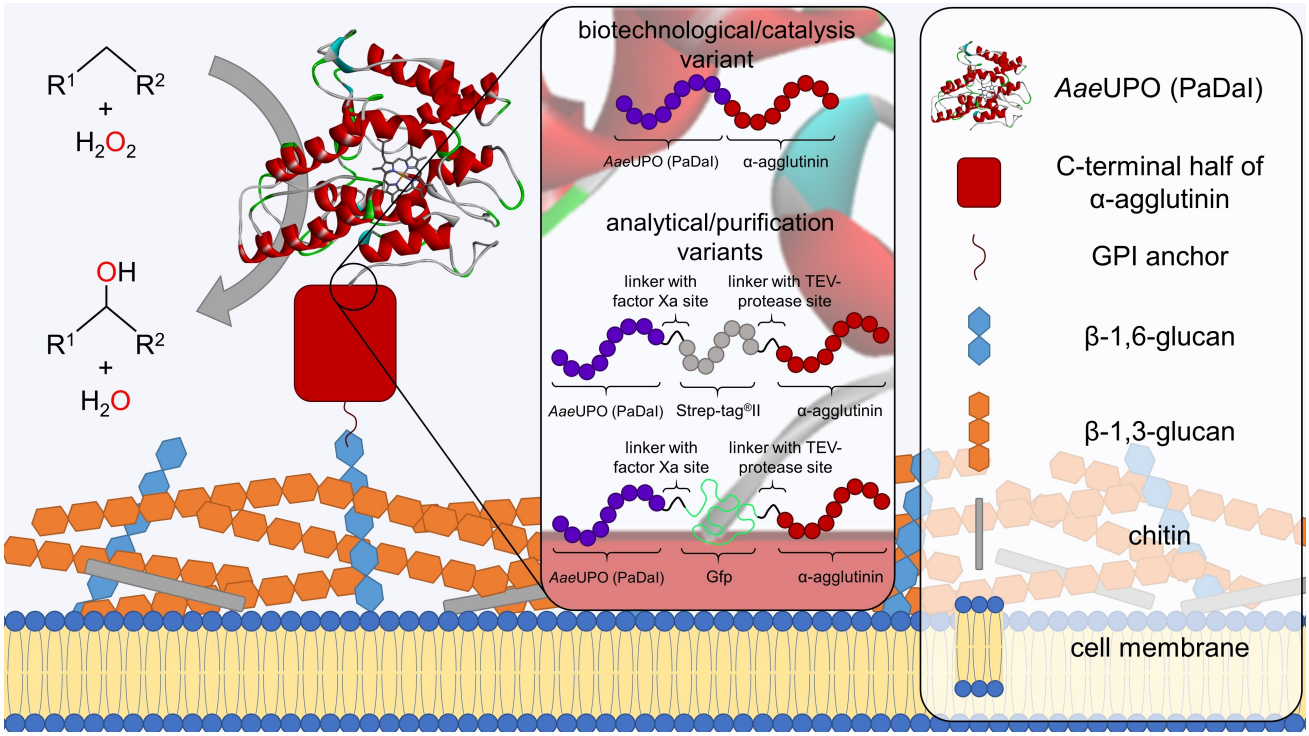

Scheme 1. Schematic Illustration of the cell surface of *Komagataella phaffii* with *Aae*UPO-PaDa–I displayed via the α-agglutinin system. The area of the fusion of PaDa–I with the C-terminal half of α-agglutinin is highlighted to showcase differences between variants for catalysis and variants for analysis and purification.

method with high activity yield, pushing biocatalytic processes with UPOs towards economic feasibility.

Results and Discussion

Construction and Cultivation of Yeast Strains with Surface Displayed UPOs

We constructed eight plasmids for surface display of *Aae*UPO-PaDa–I on *K. phaffii*, fusing parts of *SAG1*, *AGA2*, *PIR1* or one of four parts of *FLO1* (see Materials and Methods for details) from *S. cerevisiae* with the *PaDa-I* gene. In case of the *AGA2* plasmid, a second expression cassette with *AGA1* was introduced into the plasmid (Figure 1a). Although only 7 systems were originally planned, cloning of the *PIR1* based system unintentionally yielded an additional *PIR1* based system, featuring a truncated version of Pir1. The *FLO1-1326* system (using 1326 amino acids of Flo1 as anchor) bearing plasmid was confirmed after transformation in *E. coli* by sanger sequencing and colony PCR but could not be confirmed after *K. phaffii* transformation in any investigated clone by colony PCR, leaving seven systems for functional analysis.

Cultures of the seven *K. phaffii* strains and a control strain, producing secreted PaDa–I, were grown in shaking flasks for 48 h before inducing production of UPO by changing the carbon source from glycerol to methanol for additional 53 h of cultivation. Details about nomenclature for genes, proteins,

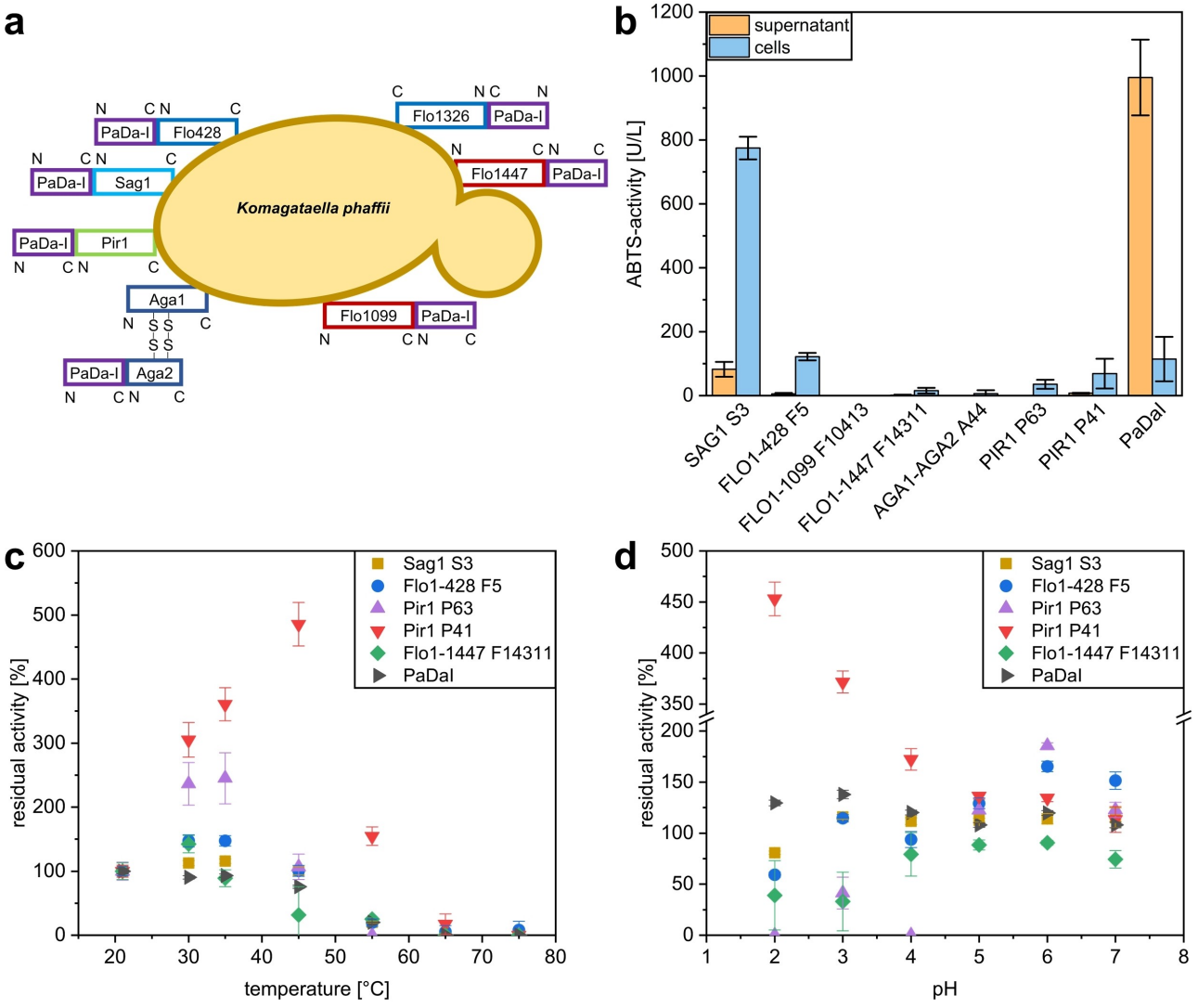

Figure 1. a: Overview about the designed surface display systems. GPI-anchored systems are displayed in blue, Pir protein systems in green and non-covalently linked systems in red. b: Activity screening of surface display systems and secreted PaDa–I. ABTS-activity of the supernatant (orange) and cells (blue) was measured individually at 30 °C after centrifugation of the cultivation broth samples and normalized to the volume of used culture. Data is labeled by the surface display system name, followed by a unique clone number or "PaDa–I" for secreted PaDa–I. For all systems, data of the best performing clone is shown (≥ 12 clones). Standard deviation (n = 3, technical replicates) is indicated. c: Thermostability of surface display systems. Residual activity at 30 °C after 1 h incubation at different temperatures in 20 mM KP_i pH 7. 100 % activity is defined as the activity at room temperature without incubation (data points at 21 °C). Standard deviation (n = 3, technical replicates) is indicated. d: pH-stability of surface display systems. Residual activity at 30 °C after 1 h incubation in different pH McIlvaine buffer (100 mM). 100 % activity is defined as activity after 1 h incubation in 20 mM KP_i pH = 7 at room temperature. Standard deviation (n = 3, technical replicates) is indicated.

strains and YSD systems are described in the supporting information.

Activity Screening

Samples from the culture broth were centrifuged and both the filtered supernatant and resuspended cells were screened for activity in a photometric assay (Figure 1b). The activity was normalized to the volume of used culture broth for comparison between surface displayed and free UPO (non-normalized data of YSD systems at $OD_{600} = 50$ can be found in Figure SI 1). All screened systems except for the FLO1-1099 system (using 1099 amino acids of Flo1 as anchor) show ABTS-activity in the resuspended cell pellet and little to no activity in the supernatant, indicating a successful surface display. Quantitatively, most systems activity of < 150 U L^{-1} cannot compete with the established production of secreted PaDa–I, which reached a volumetric activity of 1000 ± 120 U/L in the supernatant of this cultivation. However, cells of SAG1 S3 show an activity of 770 ± 40 U L^{-1}, which is more than a six-fold increase over the next best surface display system and 80% of the volumetric activity of secreted PaDa–I. Additional volumetric activity of 82 ± 23 U L^{-1} was measured in the supernatant, indicating a 90% immobilization efficiency.

Biochemical Characterization

To evaluate the usability of yeast surface displayed PaDa–I under various process conditions, a biochemical characterization was conducted, exposing the immobilized and free PaDa–I to the stressors temperature, pH and organic cosolvents acetone, acetonitrile (ACN) and dimethyl sulfoxide (DMSO). Activities were measured either with the stressor applied (activity) or at standard assay conditions after incubating the enzymes in presence of the stressor for 1 h for temperature and pH or up to 48 h for organic cosolvents (stability).

In the temperature stability evaluation, most surface display systems performed similarly to the free PaDa–I, keeping close to 100% of their initial activity after 1 h incubation at up to 45 °C but losing over 90% of it at 55 °C (Figure 1c). Contrary, the PIR1 systems were seemingly activated by incubation at temperatures up to 55 °C with an activity maximum after incubation at 45 °C (500% of initial activity). During temperature dependent activity characterization, most YSD systems as well as the free PaDa–I enzyme showed a near linear increase in activity with increasing temperature up to 75 °C and a decrease at 85 °C (Figure SI 2).

The pH-stability (Figure 1d) of most surface display systems was worse for incubation at pH 2–4 than that of free PaDa–I, which remained between 100 and 138% activity over the investigated pH range. SAG1 showed above 75% residual activity after incubation at any tested pH. PIR1 P41 experienced an activation at low pH values with a maximum of 450% residual activity after 1 h incubation at pH 2. During pH-dependent activity characterization (Figure SI 3), the SAG1 system showed near identical pH dependency to free PaDa–I. Comparatively, the PIR1 systems and FLO1-428 experienced a slight basic shift of the pH optimum. FLO1-1447 showed a narrower active pH range than the other systems.

The activity and stability in organic cosolvents are key parameters for the use of unspecific peroxygenases because many relevant substrates have low water solubility. Organic cosolvents can cause the loss of the water-shell bound to the protein surface by H-bonds[19] which plays an important role in the protein structure. Additionally, organic solvents can disrupt hydrophobic interactions between side chains of amino acids in the protein.[20] A change in structure often results in reduced activity and denaturation of the enzyme is possible.[19a] However, organic solvents can also lead to increased k_{cat} values by increasing the substrate availability of poorly water-soluble substrates. We used the well water-soluble ABTS for the activity characterization to disregard the substrate availability factor and measure enzyme activity and stability as a function of organic cosolvent concentration (Figure 2a–c).

The activity of free PaDa–I decreased with increasing concentrations of acetone, ACN and DMSO as expected and reached 50% relative activity (C_{50}) at 9%, 7% and 1% (v/v), respectively (Figure 2a–c). This is in line with results from Martin-Diaz and coworkers.[19b] SAG1 performed slightly better with C_{50} values of 9%, 9% and 1.5%. FLO1-1447 showed poor relative activity in the presence of acetone and ACN but tolerates high DMSO concentrations with a C_{50} of 10%. Contrary, the other FLO1 based system FLO1-428 performed well in acetone up to 15% with a C_{50} of 18% and near identical to SAG1 in ACN. The *PIR1* based systems experienced stronger changes in relative activity compared to other systems. Overall, PIR1 P41 showed exceptionally high activity in the tested organic solvents while PIR1 P63 was the worst performing system in ACN but the best performing system in DMSO. PIR1 P41 showed especially unexpected behaviour in increasing concentrations of acetone, where an activation to 140%–160% activity and still 100% of activity was observed in concentrations from 5%–15% and up to 25% acetone, respectively, while all other tested systems showed slight to medium inhibition in concentrations of just 5% acetone.

Besides activity, stability of the enzyme in 50% organic cosolvents was investigated (Figure SI 4–6). Free PaDa–I experienced a hyperactivation after short time incubation in 50% Acetone as described before[11b,19b] but activity decreased over time afterwards. The YSD systems did not experience this hyperactivation and their activity decreased in a similar rate as free PaDa–I and rather uniformly among all systems. The systems SAG1, FLO1-428 and PIR1 P41 were highly stable in acetone. However, stability in acetonitrile was poor for all YSD systems. SAG1 and PIR1 P41 were the exceptions here, still producing 15% and 37% residual activity after 24 h, respectively. Contrary to the ACN incubation, all YSD systems performed at least as well as the free enzyme in DMSO. PIR1 P41 was activated the most and reached 200% residual activity after 48 h.

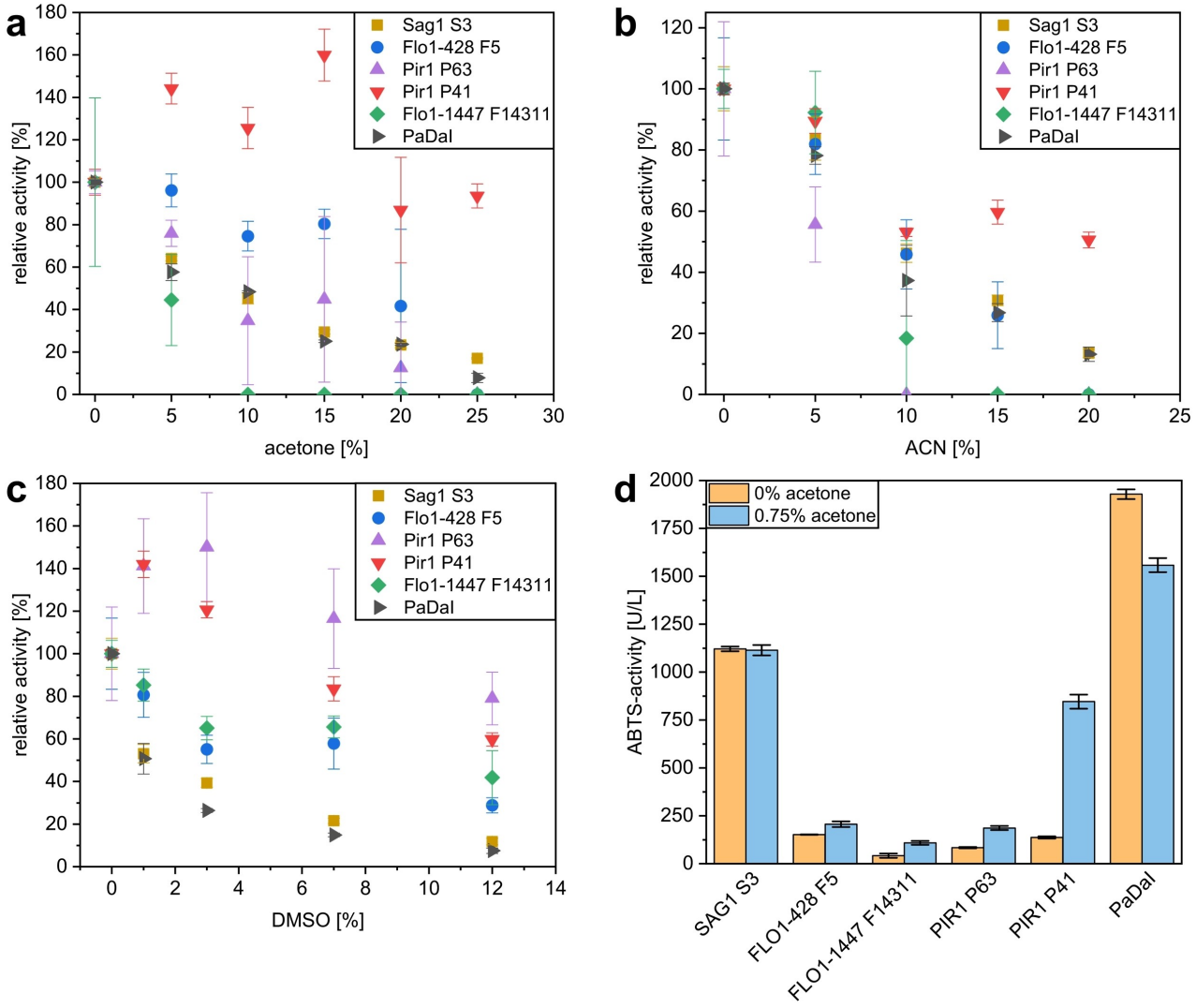

Figure 2. Biochemical characterization of the influence of organic cosolvents on the ABTS activity of surface displayed *Aae*UPO PaDa–I. Cells were resuspended in 20 mM KP_i pH = 7 before introduction to organic cosolvents and measurements were performed at 30 °C for 90 s. a: relative activity dependent on percentage of acetone present. Standard deviation (n = 3, technical replicates) is indicated. b: relative activity dependent on percentage of acetonitrile present. Standard deviation (n = 3) is indicated. c: relative activity dependent on percentage of DMSO present. Standard deviation (n = 3, technical replicates) is indicated. a–c: 100 % activity is defined as activity with no organic solvent present. d: total activity of surface display systems and free PaDa–I with and without 0.75 % acetone present. Standard deviation (n = 3, technical replicates) is indicated.

Results for temperature and pH dependent activity characterization and stability in 50 % organic cosolvents can be found in the supporting information (Figure SI 2–6).

During cosolvent stability evaluation (Figure SI 4–6), we defined 100 % residual activity by mixing free enzyme or cells with surface displayed UPOs with the cosolvent to a concentration of 50 % (v/v) and immediately taking a sample. This was done to account for the small amounts of organic cosolvent introduced to the assay by sampling (0.75 % cosolvent in the assay). However, we noticed strong changes of total activity between 0 % and 0.75 % acetone in the assay so we compared these conditions separately with cells from another cultivation of the *Komagataella* strains (Figure 2d). While the SAG1 system was not influenced by this small amount of acetone, all other systems show changes in activity. Free PaDa–I was slightly inhibited while the other YSD systems were activated. Especially PIR1 P41 was activated to around 6-fold activity in presence of 0.75 % acetone.

The activation mechanism of the PIR1 systems by moderate temperatures, low pH values and some organic cosolvents is intriguing, especially because the activated PIR1 P41 achieves total activities per culture volume close to SAG1. In case of a misfolded UPO the stressor could be responsible for a refolding process of the enzyme, causing actual activation. Alternatively, an apparent activation due to the PIR1 anchor mechanism is feasible. Contrary to the other systems, PIR1 attaches to the ß-1,6-glucan, making up around 80 % of total ß-glucans of the yeast cell surface. Enzymes attached to lower glucan layers, initially diffusion limited by the upper layers, could then be exposed if the stressors damage the cell wall. However, elucidating the mechanism is not the focus of this work.

Based on the activity screening and biochemical characterization, the PaDa–I-SAG1 system was identified as the overall most suitable system for industrial biocatalysis. During biochemical characterization, PIR1 P41 reached total activities close to SAG1 under certain conditions as described above. Based on the presented results, the existence of process parameters where the PIR1 P41 system exhibits higher activities than the SAG1 system cannot be ruled out. However, we focused on SAG1 here due to its high total activity without activation and under exposition to the tested stressors. To broaden its use cases and for further analysis, two variants of the SAG1 system were created, featuring a Strep-tag®II or Gfp-tag between the SAG1 anchor and PaDa–I. The tags are flanked by linkers with specific protease cleavage sites, allowing for separation of PaDa–I from the anchor protein, either with attached tag or without. The best performing *K. phaffii* PaDa–I_Gfp_SAG1 and *K. phaffii* PaDa–I_Strep-tag®II_SAG1 clones reached volumetric ABTS-activities of 745 $U\,L^{-1}$ and 3510 $U\,L^{-1}$ (normalized to the culture volume) in shaking flask cultivation, respectively. The control *K. phaffii* PaDa–I_SAG1 reached 1255 $U\,L^{-1}$ in this cultivation. Notably, the activity is higher with the added Strep-tag®II but slightly lower with added Gfp. We attribute these differences to further distance to the cell wall and increased mobility by the small Strep-tag®II–linker and decreased mobility by the comparatively bulky structure of Gfp.

Determination of YSD Key Parameters

To determine how much PaDa–I is immobilized per gram cell dry weight (CDW), cell dry weight was measured by drying defined volumes of cell suspension with OD_{600} of 40 and in a second experiment, PaDa–I_Strep-tag®II was cleaved from cells, displaying PaDa–I_Strep-tag®II_SAG1 for subsequent protein purification and determination (Figure SI 7–9). Key parameters of the YSD of PaDa–I with SAG1 were calculated and are summarized in Table 1. The calculated key parameters apply for this paper but it has to be assumed, that they vary between different cultivation strategies for *K.* phaffii PaDaI_SAG1.

Table 1. Key parameters of SAG1-immobilized PaDaI on *K. phaffii* X33 cells. Measurement uncertainty (error propagated) is indicated. Protein amounts are given in BSA equivalents due to Bradford protein determination methodology.

g CDW L^{-1} OD^{-1}	0.89 ± 0.03
U g CDW^{-1}	29.5 ± 1.9
µg PaDa–I g CDW^{-1}	85 ± 10
nmol PaDa–I g CDW^{-1}	1.58 ± 0.18
Specific activity U_{ABTS} mg^{-1}	346 ± 46
µg PaDa–I L^{-1} OD^{-1}	75 ± 9
U L^{-1} OD^{-1}	26.15 ± 1.4
nmol PaDa–I L^{-1} OD^{-1}	1.40 ± 0.17

Fluorescence Microscopy Results

K. phaffii PaDa–I_Gfp_SAG1 was investigated by fluorescence microscopy (Figure 3) to confirm the immobilization location on the cell surface and success of cleavage of tagged protein from the cells via TEV-protease digestion, that was used for the key parameter determination (see above).

The microscopy images showcase the distribution of Gfp-tagged PaDa–I in and on the cells of *K. phaffii*, where the majority of fluorescence is around the outside of the cell. This indicates a successful surface display of PaDa–I, not accumulating fusion protein inside the cells. After digestion with TEV-protease for 72 h, the Gfp-tagged PaDa–I was nearly completely cleaved from the cells. After TEV-protease digestion, the cells were washed 3 times with KP_i buffer and subsequently resuspended for an activity measurement. 15% of the cells initial activity remained after cleavage of the displayed enzymes.

Repeated Batch Catalysis

To demonstrate the reusability of the immobilized PaDa–I and applicability for poorly water-soluble substrates, we performed repeated batch experiments using cyclohexane as substrate. The poor solubility necessitated addition of organic cosolvent to facilitate substrate availability to the enzyme. Addition of 30% acetone yielded the highest product formation in a screening of different acetone percentages from 0–50% (data not shown) even though, the enzymes activity is strongly inhibited at this concentration (see Figure 2a). For each 20 mL reaction system, 12.92 mL of *K.p.* X33 pPpB1_PaDa–I_SAG1 (100 ± 4 $U_{ATBS}\,mL^{-1}$) in 100 mM KP_i pH = 6.9, 6 mL acetone and 1.08 mL cyclohexane were added into a 50 mL reaction vessel and inverted for 20 h per batch at room temperature. 2 mL of

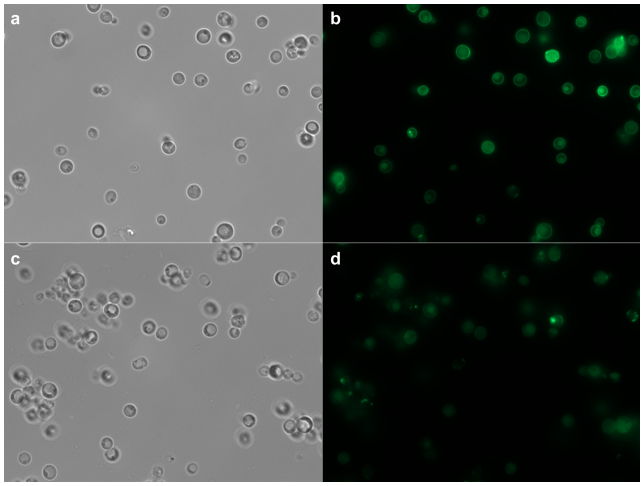

Figure 3. Differential interference contrast (DIC) and fluorescence microscopic analysis of *K. phaffii* PaDa–I_Gfp_SAG1 cells. a: DIC microscopy image of untreated cells. b: fluorescence microscopy of untreated cells. c: DIC microscopy image of cells after 72 h of TEV-protease digestion. d: fluorescence microscopy image of cells after 72 h of TEV-protease digestion.

100 mM H_2O_2 were added via a syringe pump over the 20 h (200 μmol per batch). After each batch, the cells with displayed UPO were separated from the reaction medium via centrifugation and subsequently resuspended in 100 mM KP_i pH = 6.9 to a volume of 12.92 mL and mixed with 6 mL acetone and 1.08 mL cyclohexane for the next batch. The hydroxylation- and overoxidation products cyclohexanol and cyclohexanone were quantified at the start and end of each batch (Figure 4).

Catalysis with the immobilized PaDa–I was highly reproducible between the 4 replicates and product selectivity for the alcohol was 97%. Over the 13 conducted batches, performance improved within the first 6 batches to a maximum of 67.1 ± 2.8 μmol (n = 4) of cyclohexanol and 1.13 ± 0.05 μmol (n = 4) of cyclohexanone. Performance decreased rapidly after 9–10 conducted batches, setting the usable catalysis duration to around 200 h. We attribute the performance increase between batches to organic cosolvent-linked activation mechanisms described earlier. Overall, 529 ± 7 μmol (53.0 ± 0.7 mg; n = 4) of cyclohexanol and 17 ± 2 μmol (1.7 ± 0.2 mg; n = 4) cyclohexanone were found after 13 batches, resulting in a productivity of 9.56 ± 0.15 $mg_{product}\,h^{-1}\,L^{-1}$. Productivity for batch 6 was 14.3 ± 0.9 $mg_{product}\,h^{-1}\,L^{-1}$. While this is still far lower than what is considered industrially relevant, the aim of this experiment was not an optimization of productivity but rather a demonstration of the immobilization of PaDa–I by yeast surface display.

At the end of batch 13, the OD_{600} of the cells, resuspended to a volume of 12.92 mL was 430 ± 30 (n = 4) so OD_{600} decreased by 35% from the original 660, likely due to a combination of cell disruption and accumulation of small losses during centrifugation and transfer to new reaction vessels between batches. However, ABTS activity of the cell suspension decreased from initially 100 ± 4 $U\,mL^{-1}$ to 0 $U\,mL^{-1}$ (n = 4) so inactivation of the enzymes was the primary cause for decrease in catalysis efficiency after batch 10. Based on the amount of immobilized PaDaI per gram CDW, a total turnover number (TTN) of 3.57•10^5 and k_{cat} of 0.38 s^{-1} was calculated. The loss of cells was not accounted for so the given values are likely underestimating the enzymes performance slightly.

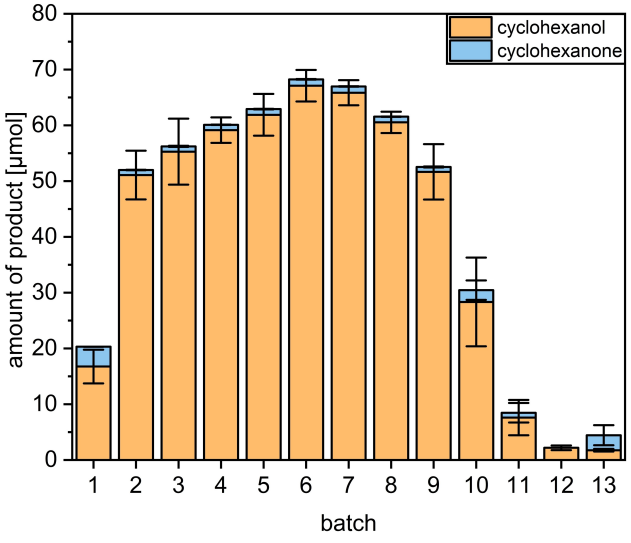

Figure 4. Analysis of repeated batch catalysis of cyclohexane hydroxylation. The amounts of the hydroxylation and overoxidation product cyclohexanol and cyclohexanone were determined before and after each batch and produced amount of substance is shown (blue and orange columns). Standard deviation (n = 4, independent experiments) is indicated.

Discussion

We constructed several yeast surface display systems for the display of *Aae*UPO PaDa–I on the cell surface of *Komagataella phaffii* for cheap immobilization with high activity yields. A display via SAG1 anchor offers excellent activity yields of 80% and the downstream processing after yeast fermentation to receive immobilized biocatalyst is easier and quicker than in previous studies[8,11a,12,13] and even easier than producing pure, free enzyme.[7a,21] In a repeated batch experiment, the immobilization method provided easy separation of the biocatalyst from the reaction medium by centrifugation. Additionally, high total turnover numbers were reached by the immobilized PaDa–I, even though the reaction setup is rather simple. Since H_2O_2 was fed per syringe pump while mixing, we expected low deactivation of the enzyme because concentration hotspots are avoided unlike with drop in-feeds as reported elsewhere.[22] We attribute the high activity yield to multiple factors. Firstly, expression and secretion of the fusion protein of PaDa–I and SAG1 is likely comparable to those of free PaDa–I because we were able to use the secretion signal of PaDa–I which has been optimized for the secretion in *K. phaffii*.[11b] Additionally, diffusion limitations are minimal for YSD immobilization because the size of each immobilization carrier particle is much smaller than that of most conventional carriers and ii. due to the molecular display, the vast majority of PaDa–I is displayed on the outside of the carrier as has been shown by fluorescence microscopy. Contrary, conventional immobilization carriers are often porous and enzymes in the pores are usually diffusion limited.[23] Unlike many other enzymes that were immobilized via YSD, PaDa–I did not experience significant improvements in stability against various stressors.[24] However, PaDa–I is already a highly stable enzyme due to its secreted nature and high degree of glycosylation.

While the immobilization on the producing yeast cells is likely the lowest cost immobilization method, the principle does come with limitations compared to conventional carriers. The yeast cells are susceptible to shear forces and less stable against high temperatures, solvents, and extreme pH values. Since one of the advantages of enzymatic biocatalysis over alternative production routes is the mild reaction conditions, we deem these factors to be negligible if the reaction parameters allow for the cells to remain intact longer than the biocatalyst. The small size of yeast cells can lead to practical issues because they are harder to retain than bigger particles and membranes with small enough pore size tend towards clogging and fouling.[25] Since the yeast cells are not killed before use, some complications could appear due to the bioactive nature of this immobilization carrier. Substrates can theoretically be imported into the cells and metabolized or adhere to the cell surface, although in the case of displayed UPOs, most relevant

substrates are not typical yeast metabolites. Additionally, reaction conditions can lead to biological stress responses such as autolysis, influencing the carrier structure and introducing impurities to the product. However, stress response in budding yeasts is a well-researched field and construction of stress tolerant yeast strains is established.[26]

Conclusions

This study presents for the first time an immobilization method for the model UPO *Aae*UPO PaDa–I with good activity yields while additionally simplifying downstream process effort. Overcoming this crucial cost-bottleneck will contribute to industrial biobased production processes with UPOs gaining economic attraction, especially for the production of bulk chemicals. Consequently, scale-up and experiments under discrete industrially relevant conditions are required to progress development of such processes. In the upcoming years we expect to see further advances in the development of suitable reaction conditions, reactor types, bio-compatible solvents and possibly water free catalysis with this type of immobilized UPOs for substrates beyond the ones here showcased.

Experimental Section

Strain Construction

The integration vector pPpB1_*Aae*UPO_PaDa–I was amplified from gDNA of *K. phaffii* strain X33_pPpB1_*Aae*UPO_PaDa–I, provided by Sebastian Bormann and circularized by subsequent T4 polynucleotide kinase and T4 ligase incubation. Three linear versions of the vector were created via whole plasmid amplification for insertion of anchor genes upstream or downstream of the *PaDa-I* gene or insertion of a secondary expression operon with *AGA1*. The *Saccharomyces cerevisiae* strains CEN.PK2 and FY1679-01B were purchased from Euroscarf and their gDNA was isolated via isopropanol precipitation and washed with ethanol. Gene fragments of the anchor protein genes for insertion into the integration vector were amplified either directly from the gDNA or if necessary, the entire gene was amplified from gDNA first and the fragment of interest subsequently amplified from the isolated gene. *SAG1*, *AGA1* and *AGA2* were isolated from CEN.PK2 gDNA and *PIR1* and *FLO1* were isolated from FY1679-01B gDNA. Eight surface display integration vectors were constructed from these fragments via Gibson assembly: I) 3′ 960 bp of *SAG1* downstream of *PaDa-I*. II) 3′ 1284 bp of *FLO1* downstream of *PaDa-I*. III) 3′ 3978 bp of *FLO1* downstream of *PaDa-I*. IV) 5′ 4341 bp of *FLO1* upstream of *PaDa-I*. V) 5′ 3297 bp of *FLO1* upstream of *PaDa-I*. VI) 3′ 834 bp of *PIR1* downstream of *PaDa-I*. VII) 3′ 834 bp of *PIR1* downstream of *PaDa-I* with deletion of bp 145–387, coding for Q112-G192 of PIR1. VIII) *AGA2* downstream of *PaDa-I* and an additional operon consisting of *AOX1* promoter, *AGA1* and *AOX1* terminator upstream of the *PaDa-I* operon. Notably, the construction of VII) was an unintentional byproduct of the construction of VI) and the deletion was only later discovered and determined during colony PCR and sequencing. Since the deletion caused no frameshift and PIR1 has multiple anchor points to the yeast cell wall, we decided to proceed with this truncated version of *PIR1* additionally to the originally intended version. The vectors were transformed into chemically competent *E. coli* NEB α and cells were plated on LB-agar + 25 μg mL^{-1} zeocin. Colonies were picked into 30 μL sterile H_2O and integration of the anchor protein gene sequence was confirmed via colony PCR. Positive clones were cultivated in LB medium + 25 μg mL^{-1} zeocin for multiplication of the plasmid and correct assembly was confirmed by sanger sequencing after plasmid preparation. Isolated, *E. coli* borne plasmids were linearized with PstI-HF for II, III and VI or with DrdI for I, IV and V for transformation into electrocompetent *K. phaffii* X33 cells which were plated on YPDS agar + 100 μg mL^{-1} zeocin. Colonies were picked both in 30 μL sterile H_2O and YPD + 100 μg mL^{-1} zeocin, the suspension in H_2O was incubated at 99 °C for 10 min and −80 °C for 20 min to disrupt the cells and integration of the plasmid was confirmed via colony PCR. Cryo-stocks were prepared from the cell suspensions in YPD after incubation at 30 °C and positive colony PCR.

Cultivation of *Komagataella phaffii* for Surface Display of UPOs

For the activity screening *K. phaffii* strains were cultivated in a 3 mL preculture in YPD medium + 100 mg mL zeocin at 30 °C, 200 rpm until stationary phase. From them, 100 mL shaking flasks with 18 mL BMG medium (100 mM KP_i pH 6, 10 g L^{-1} yeast extract, 20 g L^{-1} peptone, 10 g L^{-1} glycerol, 400 μg L^{-1} biotin, 3.2 mM $MgSO_4$, 1.7 g L^{-1} yeast nitrogen base without amino acids, 10 g L^{-1} $(NH_4)_2SO_4$) + 100 μg mL^{-1} zeocin were inoculated with the preculture to an optical density of 0.1 and incubated at 30 °C, 200 rpm. After incubation for 48 h until stationary phase, 2 mL BMMY medium (100 mM KP_i pH 6, 10 g L^{-1} yeast extract, 20 g L^{-1} peptone, 5 g L^{-1} methanol, 400 μg L^{-1} biotin, 3.2 mM $MgSO_4$, 1.7 g L^{-1} yeast nitrogen base without amino acids, 10 g L^{-1} $(NH_4)_2SO_4$) + 100 μg mL^{-1} zeocin were added for methanol acclimatization. 8 h after acclimatization a methanol feed of 1% (v/v) methanol per day (66 μL in the morning, 134 μL in the evening) was started. Twice a day samples were taken, centrifuged, supernatant filter sterilized, and cell pellet resuspended in 20 mM KP_i pH 7 to an optical density of 100. ABTS (2,2′-azino-bis(3-ethylbenzothiazoline-6-sulfonic acid)) activity of supernatant and cells were measured and the cultivation was terminated when ABTS activity did not increase between measurements by centrifuging the entire culture and treating supernatant and cells like described above and stored at −20 °C.

Larger scale production of *K. phaffii* with displayed PaDa–I_SAG1, PaDa–I_His_6_SAG1 and PaDa–I_Gfp_SAG1 from precultures were incubated in baffled, 1 L shaking flasks in 100 mL BMG + 100 μg mL^{-1} zeocin until optical density reached 25. Cultures were centrifuged and cell pellets resuspended in 50 mL BMMY + 100 μg mL^{-1} zeocin each and incubated in 500 mL baffled shaking flasks with methanol feed as described above.

Activity Assays

The oxidation of ABTS to a stable radical by the peroxidase activity of PaDa–I was routinely used as activity assay. The assay consisted of 100 μL 3 mM ABTS in McIlvaine buffer pH 4.5, 100 μL of free enzyme or cells to a final optical density of 0.5 in the assay, 50 μL of 40 mM H_2O_2 and McIlvaine buffer pH 4.5 to a total volume of 1 mL. The reaction was started by addition of the H_2O_2 and the absorbance at 420 nm was measured. Activity was calculated via the extinction coefficient of ABTS $\varepsilon_{420} = 36000\ M^{-1}cm^{-1}$. For comparison of the activity of free enzyme with surface displayed enzyme, activities were normalized to culture volume during the activity screening by correcting the measured activity of the cells by the ratio of the optical density of the culture and the optical density the cells were stored at.

Repeated Batch Experiments

Repeated batch experiments were conducted in 50 mL Falcon tubes at room temperature and inverted in a back- and forth motion (program F7) at 60 rpm in a Intelli-Mixer (NeoLab, Heidelberg, Germany) for 20 h per batch. The bottles were filled with 12.92 mL *K.p.* X33 pPpB1_PaDa–I_SAG1 cells, resuspended in 100 mM KP_i pH = 6.9 to an optical density of 660 (ABTS activity of 100 ± 4 U mL^{-1}). 6 mL acetone and 1.08 mL cyclohexane were added and the catalysis was started by starting a H_2O_2 feed via syringe pump with 100 μL h^{-1} of 100 mM H_2O_2 for 20 h. At the start and end of each batch, 500 μL samples were taken, extracted with 250 μL of ethyl acetate with 10 mM 1-octanol and centrifuged. 150 μL of the ethyl acetate phase was taken for GC analysis. The cell pellet was resuspended to a volume of 500 μL in KP_i pH = 6.9 and reintroduced into the reaction vessel. At the end of each batch, the entire reaction volume was centrifuged and the cell pellet was resuspended to a volume of 12.92 mL with 100 mM KP_i pH 6.9 and stored at 4 °C until the next batch (< 4 h to run 1 batch d^{-1}).

Quantification of Cyclohexanol and Cyclohexanone

Identification and quantification of cyclohexanol and cyclohexanone from the repeated batch experiments was done by GC. Extraction of the 500 μL samples was done with 250 μL ethyl acetate with 10 mM 1-octanol as internal standard by rigorously mixing the phases via vortex mixer, letting the samples rest for a minimum of 2 min, centrifuging and subjecting the supernatant (ethyl acetate phase) to GC analysis (Agilent DB-WAX 30 m, 0.25 mm, 0.25 μm; 1 μL injection; 10:1 split ration; 40 °C for 5 min, 25 °C min^{-1} to 250 °C, 250 °C for 5 min; detection via flame ionization detector). Quantification was done via a calibration curve of standards with identical sample preparation and using 1-octanol as internal standard ($R^2 = 0.999$ for cyclohexanol; $R^2 = 0.995$ for cyclohexanone).

Determination of YSD Parameters

For determination of the amount of PaDa–I per gram of cell dry weight, 5 mL of a suspension of *K. phaffii* PaDa–I_Gfp_SAG1 and *K. phaffii* PaDa–I_Strep-tag®II _SAG1, adjusted to OD_{600} of 50 (222 ± 7 mg CDW) were centrifuged and the cell pellet resuspended to a volume of 2 mL with TEV-protease buffer (50 mM Tris-HCl, 0.5 mM EDTA, 1 mM DTT, pH = 7.5) each. 100 μL of TEV-protease (10000 U mL^{-1}, New England Biolabs) was added to each cell suspension and the mixture was incubated at 25 °C for 72 h and sampled at 24 h, 48 h and 72 h. *K. phaffii* PaDa–I_Gfp_SAG1 suspension was centrifuged and the cells washed twice with 100 mM KP_i pH = 7 before fluorescence microscopy to confirm, that the PaDa–I_Gfp was fully detached from the cells after TEV-protease digestion. The *K. phaffii* PaDa–I_Strep-tag®II_SAG1 suspension was centrifuged, the cell pellet washed 4 times with 1 mL H_2O and the supernatant and wash fractions (in opposite order than obtained) were subjected to Strep-tag®II purification via a gravity flow column according to the manufacturers protocol (IBA Lifesciences, Göttingen, Germany). The elution fraction with the highest activity was then concentrated and the buffer was changed to his-tag binding buffer (20 mM sodium phosphate, 300 mM NaCl, pH 7.4) via a Microcon® 10 centrifugal filter (Merck, Darmstadt, Germany). Then, his-tag purification was done with a NEBExpress® Ni-Spin column according to the manufacturers protocol to remove TEV-protease contamination. Protein amount in the flowthrough was determined via a modified Bradford-Assay with ROTI®Nanoquant (Carl Roth, Karlsruhe, Germany) using bovine serum albumin fraction V as reference protein ($R^2 = 0.999$). Throughout the purification, ABTS activity was routinely measured after each step to determine the associated yield. After Strep-tag®II purification and after his-tag purification, SDS-PAGEs were conducted to track purity of the samples (Figure SI 6 + 7). The measured protein amount was corrected with the yields of each purification step (Figure SI 8) and correlated to the CDW of the cells it was cleaved from. The resulting protein amount per CDW was divided by the size of the cleaved PaDaI_Strep-tag®II (51.1 kDa for PaDaI and 2.84 kDa for the linker and Strep-tag®II) to yield the molar amount of enzyme per gram CDW. Using this and the activity per gram CDW, the specific activity of the immobilized PaDaI_Strep-tag®II was calculated and used to determine TTN and k_{cat} of the repeated batch experiments.

Acknowledgements

We acknowledge support and funding by the Deutsche Forschungsgemeinschaft (DFG, German Research Foundation, project 465474720). We also kindly thank Prof. Dr. Reinhard Fischer and Michael Pitz for granting access to and helping with fluorescence microscopy. Open Access funding enabled and organized by Projekt DEAL.

Conflict of Interests

The authors declare no conflict of interest.

Data Availability Statement

The data that support the findings of this study are available from the corresponding author upon reasonable request.

Keywords: Immobilization · Enzyme catalysis · Unspecific peroxygenases · Yeast surface display

[1] a) M. Hobisch, D. Holtmann, P. Gomez de Santos, M. Alcalde, F. Hollmann, S. Kara, *Biotechnol. Adv.* **2021**, *51*, 107615; b) S. Bormann, A. Gomez Baraibar, Y. Ni, D. Holtmann, F. Hollmann, *Catal. Sci. Technol.* **2015**, *5*, 2038–2052; c) Y. Wang, D. Lan, R. Durrani, F. Hollmann, *Curr. Opin. Chem. Biol.* **2017**, *37*, 1–9.
[2] M. Kinne, M. Poraj-Kobielska, E. Aranda, R. Ullrich, K. E. Hammel, K. Scheibner, M. Hofrichter, *Bioorg. Med. Chem. Lett.* **2009**, *19*, 3085–3087.
[3] C. Aranda, R. Ullrich, J. Kiebist, K. Scheibner, J. C. del Río, M. Hofrichter, A. T. Martínez, A. Gutiérrez, *Catal. Sci. Technol.* **2018**, *8*, 2394–2401.
[4] S. Peter, M. Kinne, X. Wang, R. Ullrich, G. Kayser, J. T. Groves, M. Hofrichter, *FEBS J.* **2011**, *278*, 3667–3675.
[5] Y. Ni, E. Fernandez-Fueyo, A. Gomez Baraibar, R. Ullrich, M. Hofrichter, H. Yanase, M. Alcalde, W. J. van Berkel, F. Hollmann, *Angew. Chem. Int. Ed. Engl.* **2016**, *55*, 798–801.
[6] A. Gutierrez, E. D. Babot, R. Ullrich, M. Hofrichter, A. T. Martinez, J. C. del Rio, *Arch. Biochem. Biophys.* **2011**, *514*, 33–43.
[7] a) F. Tonin, F. Tieves, S. Willot, A. van Troost, R. van Oosten, S. Breestraat, S. van Pelt, M. Alcalde, F. Hollmann, *Org. Process Res. Dev.* **2021**, *25*, 1414–1418; b) T. Hilberath, R. van Oosten, J. Victoria, H. Brasselet, M. Alcalde, J. M. Woodley, F. Hollmann, *Org. Process Res. Dev.* **2023**, *27*, 1384–1389.
[8] S. Bormann, B. O. Burek, R. Ulber, D. Holtmann, *J. Mol. Catal.* **2020**, *492*, 110999.
[9] J. M. Bolivar, J. M. Woodley, R. Fernandez-Lafuente, *Chem. Soc. Rev.* **2022**, *51*, 6251–6290.
[10] P. Molina-Espeja, P. Santos-Moriano, E. García-Ruiz, A. Ballesteros, F. J. Plou, M. Alcalde, *Int. J. Mol. Sci.* **2019**, *20*, 1627.

[11] a) M. Hobisch, P. D. Santis, S. Serban, A. Basso, E. Byström, S. Kara, *Org. Process Res. Dev.* **2022**, *26*, 2761–2765; b) P. Molina-Espeja, E. Garcia-Ruiz, D. Gonzalez-Perez, R. Ullrich, M. Hofrichter, M. Alcalde, *Appl. Environ. Microbiol.* **2014**, *80*, 3496–3507.
[12] P. D. Santis, N. Petrovai, L.-E. Meyer, M. Hobisch, S. Kara, *Front. Chem.* **2022**, *10*, 985997.
[13] P. D. Santis, D. Wegstein, B. O. Burek, J. Patzsch, M. Alcalde, W. Kroutil, J. Z. Bloh, S. Kara, *ChemSusChem* **2023**, *16*, e202300613.
[14] a) J.-M. Wang, C.-M. Wang, X. Men, T.-Q. Yue, C. Madzak, X.-H. Xiang, H.-Y. Xiang, H.-B. Zhang, *Enzyme Microb. Technol.* **2020**, *135*, 109498; b) K. Ilić Đurđić, R. Ostafe, A. Đurđević Đelmaš, N. Popović, S. Schillberg, R. Fischer, R. Prodanović, *Enzyme Microb. Technol.* **2020**, *136*, 109509.
[15] a) R. Yamada, Y. Kimoto, H. Ogino, *Biochem. Eng. J.* **2016**, *113*, 7–11; b) X.-Q. Peng, *Appl. Biochem. Biotechnol.* **2013**, *169*, 351–358; c) K. Tokuhiro, N. Ishida, A. Kondo, H. Takahashi, *Appl. Microbiol. Biotechnol.* **2008**, *79*, 481–488.
[16] X. He, J. Shang, F. Li, H. Liu, *Biotechnol. Appl. Biochem.* **2015**, *62*, 1–8.
[17] Z. Qiu, H. Tan, S. Zhou, L. Cao, *Mol. Biotechnol.* **2014**, *56*, 726–730.
[18] a) C. Andreu, M. L. Del Olmo, *Appl. Microbiol. Biotechnol.* **2018**, *102*, 2543–2561; b) M. Ye, Y. Ye, Z. Du, G. Chen, *Bioproc. Biosyst. Eng.* **2021**, *44*, 1003–1019.
[19] a) P. V. Iyer, L. Ananthanarayan, *Proc. Biochem.* **2008**, *43*, 1019–1032; b) J. Martin-Diaz, P. Molina-Espeja, M. Hofrichter, F. Hollmann, M. Alcalde, *Biotechnol. Bioeng.* **2021**, *118*, 3002–3014.
[20] T. Asakura, K. Adachi, E. Schwartz, *J. Biol. Chem.* **1978**, *253*, 6423–6425.
[21] a) A. E. W. Horst, S. Bormann, J. Meyer, M. Steinhagen, R. Ludwig, A. Drews, M. Ansorge-Schumacher, D. Holtmann, *J. Mol. Catal. B: Enzymat.* **2016**, *133*, S137–S142; b) H. E. Bonfield, K. Mercer, A. Diaz-Rodriguez, G. C. Cook, B. S. J. McKay, P. Slade, G. M. Taylor, W. X. Ooi, J. D. Williams, J. P. M. Roberts, J. A. Murphy, L. Schmermund, W. Kroutil, T. Mielke, J. Cartwright, G. Grogan, L. J. Edwards, *ChemPhotoChem* **2020**, *4*, 45–51; c) S. Bormann, H. Kellner, J. Hermes, R. Herzog, R. Ullrich, C. Liers, R. Ulber, M. Hofrichter, D. Holtmann, *Antioxidants* **2022**, *11*, 223.
[22] F. Perz, S. Bormann, R. Ulber, M. Alcalde, P. Bubenheim, F. Hollmann, D. Holtmann, A. Liese, *ChemCatChem* **2020**, *12*, 3666–3669.
[23] J. Boudrant, J. M. Woodley, R. Fernandez-Lafuente, *Proc. Biochem.* **2020**, *90*, 66–80.
[24] a) Y. Peng, Y. Wang, X. Liu, R. Zhou, X. Liao, Y. Min, L. Ma, Y. Wang, B. Rao, *Molecules*, Basel, Switzerland **2022**, 27; b) M. V. H. Moura, G. P. Da Silva, A. C. D. O. Machado, F. A. G. Torres, D. M. G. Freire, R. V. Almeida, *PloS One* **2015**, *10*, e0141454; c) B. Rao, R. Zhou, Q. Dong, X. Liao, F. Liu, W. Chen, X. Liu, Y. Min, Y. Wang, *Biotechnol. Bioprocess Eng.* **2020**, *25*, 571–579; d) G.-D. Su, D.-F. Huang, S.-Y. Han, S.-P. Zheng, Y. Lin, *Appl. Microbiol. Biotechnol.* **2010**, *86*, 1493–1501; e) S. Yang, X. Lv, X. Wang, J. Wang, R. Wang, T. Wang, *Front. Microbiol.* **2017**, *8*, 2583; f) E. Y. Yuzbasheva, T. V. Yuzbashev, N. I. Perkovskaya, E. B. Mostova, T. V. Vybornaya, A. V. Sukhozhenko, I. Y. Toropygin, S. P. Sineoky, *Appl. Biochem. Biotechnol.* **2015**, *175*, 3888–3900; g) B. Shi, X. Ke, H. Yu, J. Xie, Y. Jia, R. Guo, *J. Microbiol. Biotechnol.* **2015**, *25*, 1856–1862.
[25] W. Guo, H.-H. Ngo, *J. Li, Bioresour. Technol.* **2012**, *122*, 27–34.
[26] a) N.-X. Lin, Y. Xu, X.-W. Yu, *Syst. Microbiol. Biomanufacturing* **2022**, *2*, 232–245; b) F. Estruch, *FEMS Microbiol. Rev.* **2000**, *24*, 469–486.

Manuscript received: May 24, 2024
Revised manuscript received: June 27, 2024
Accepted manuscript online: July 4, 2024
Version of record online: August 22, 2024